Traps, Patches, and Spots: Asymptotic Analysis of Localized Solutions to Some Diffusive Processes

Michael J. Ward (UBC)

PIMS Workshop: Kinetic Theory and Related Fields: November 2014

Special Workshop in Honor of Reinhard Illner

Collaborators:, D. Coombs (UBC); R. Straube (Max-Planck, Magdeburg); A. Cheviakov and R. Spiteri (U. Saskatchewan), I. Rozada (BC HIV Center Excellence), S. Ruuth (SFU), Phillipe Trinh (Oxford)

Outline of the Talk

THREE SPECIFIC (SEEMINGLY UNRELATED) TOPICS:

- **Part I (Patches):** The Mean First Passage Time (MFPT) for Diffusive Escape from a Sphere Through a Narrow Window on its Boundary.
- **Part II (Traps):** The MFPT for Diffusion on the Surface of a Sphere with Small Traps.
- **Part III (Spots):** The slow dynamics and equilibria of spot-type patterns for the singularly perturbed Brusselator RD model on the sphere.

COMMONALITIES:

1. Asymptotic reduction to discrete optimization problems for interacting “particles” (Part I, II)
2. Reduction to DAE (differential algebraic ODE) system of “interacting particles” on the sphere (Part III)
3. All are related to Fekete points

Part I: Narrow Escape Problem in 3-D

Narrow Escape: Brownian motion with diffusivity D in Ω with $\partial\Omega$ insulated except for an (multi-connected) absorbing patch $\partial\Omega_a$ of measure $O(\varepsilon)$. Let $\partial\Omega_a \to x_j$ as $\varepsilon \to 0$ and $X(0) = x \in \Omega$ be initial point for Brownian motion.

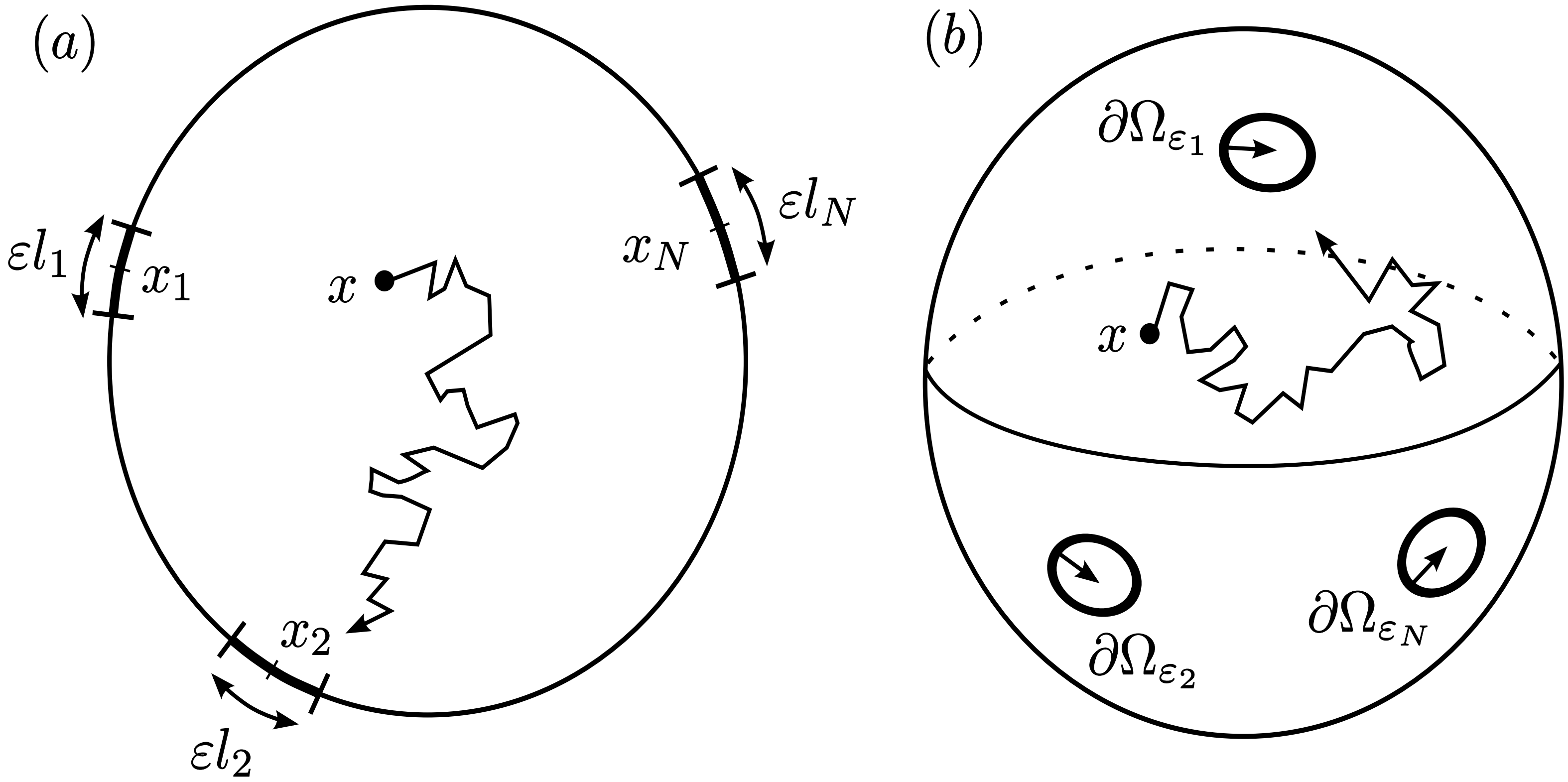

Left: 2-D **Right: 3-D**

Part I: Mathematical Formulation

The mean first passage time MFPT $v(x) = E\left[\tau | X(0) = x\right]$ for the narrow escape problem satisfies a Poisson problem with Dirichlet/Neumann boundary conditions (Z. Schuss (1980))

$$\Delta v = -\frac{1}{D}\,, \quad x \in \Omega\,,$$
$$\partial_n v = 0 \quad x \in \partial\Omega_r\,; \quad v = 0\,, \quad x \in \partial\Omega_a = \cup_{j=1}^{N} \partial\Omega_{\varepsilon_j}\,.$$

An eigenfunction expansion shows that the average MFPT $\bar{v}$ satisfies

$$\bar{v} = \frac{1}{|\Omega|} \int_\Omega v\,dx \sim \frac{1}{D\lambda_1}\,, \quad \text{as} \quad \varepsilon \to 0\,.$$

Here λ_1 is the principal eigenvalue of

$$\Delta u + \lambda u = 0\,, \quad x \in \Omega\,; \quad \int_\Omega u^2\,dx = 1\,,$$
$$\partial_n u = 0 \quad x \in \partial\Omega_r\,, \quad u = 0\,, \quad x \in \partial\Omega_a = \cup_{j=1}^{N} \partial\Omega_{\varepsilon_j}\,.$$

Since $|\partial\Omega_a| = \mathcal{O}(\varepsilon)$, then $\bar{v} \to \infty$ and $\lambda_1 \to 0$ as $\varepsilon \to 0$.

Part I: Relevance to Biophysics

KEY GENERAL REFERENCES:

- Z. Schuss, A. Singer, D. Holcman, *The Narrow Escape Problem for Diffusion in Cellular Microdomains*, PNAS, **104**, No. 41, (2007), pp. 16098-16103.
- O. Bénichou, R. Voituriez, *Narrow Escape Time Problem: Time Needed for a Particle to Exit a Confining Domain Through a Small Window*, Phys. Rev. Lett, **100**, (2008), 168105.
- S. Condamin, et al., Nature, **450**, 77, (2007)
- S. Condamin, O. Bénichou, M. Moreau, Phys. Rev. E., **75**, (2007).

RELEVANCE OF NARROW ESCAPE TIME PROBLEM IN BIOLOGY:

- time needed for a reactive particle released from a specific site to activate a given protein on the cell membrane
- biochemical reactions in cellular microdomains (dendritic spines, synapses, microvesicles), consisting of a small number of particles that must exit the domain to initiate a biological function.
- determines reaction rate in Markov model of chemical reactions

Part I: Some Previous Results

- For a 3-D domain with smooth boundary (MJW, Keller, SIAP, 1993)

$$\lambda_1 \sim \frac{2\pi\varepsilon}{|\Omega|} \sum_{j=1}^{N} C_j \,.$$

Here C_j is the capacitance of the electrified disk problem

$$\Delta_y w = 0\,, \quad y_3 \geq 0, \quad -\infty < y_1, y_2 < \infty\,; \quad w \sim C_j/|y|\,, \quad |y| \to \infty\,.$$

$$w = 1\,, \quad y_3 = 0\,, \, (y_1, y_2) \in \partial\Omega_j\,; \; \partial_{y_3} w = 0\,, \quad y_3 = 0\,, \, (y_1, y_2) \notin \partial\Omega_j\,.$$

- For one circular trap of radius ε on the unit sphere Ω with $|\Omega| = 4\pi/3$,

$$\bar{v} \sim \frac{|\Omega|}{4\varepsilon D} \left[1 - \frac{\varepsilon}{\pi} \log \varepsilon + O(\varepsilon) \right] \,,$$

Ref: A. Singer et al. J. Stat. Phys., **122**, No. 3, (2006).

- For arbitrary Ω with smooth $\partial\Omega$ and one circular trap at $x_0 \in \partial\Omega$

$$\bar{v} \sim \frac{|\Omega|}{4\varepsilon D} \left[1 - \frac{\varepsilon}{\pi} H \log \varepsilon + O(\varepsilon) \right] \,.$$

Here H is the mean curvature of $\partial\Omega$ at $x_0 \in \partial\Omega$. **Ref:** A. Singer, Z. Schuss, D. Holcman, Phys. Rev. E., **78**, No. 5, 051111, (2009).

Part I: Main Goals

Applications: Specific Scientific Questions:

- Obtain explicit higher-order asymptotics for $v(x)$ and $\bar{v}$ as $\varepsilon \to 0$.
- Determine whether there is a signficant effect on $\bar{v}$ of the spatial configuration $\{x_1, \ldots, x_n\}$ of traps.
- What is the effect on $\bar{v}$ of fragmentation of the trap set?
- Develop scaling laws for large N.

Math: Connections to Approximation Theory: Let Ω be the unit sphere with N-circular absorbing patches on $\partial\Omega$ of a common radius. Is minimizing $\bar{v}$ equivalent to minimizing the Coulomb energy $\mathcal{H}_C(x_1, \ldots, x_N)$ defined by

$$\mathcal{H}_C(x_1, \ldots, x_N) = \sum_{j=1}^{N} \sum_{k>j}^{N} \frac{1}{|x_j - x_k|}, \qquad |x_j| = 1 .$$

Such points are **Fekete points.** They correspond to finding the minimal energy configuration of “electrons” on the sphere. (References: J.J. Thomson, E. Saff, N. Sloane, A. Kuijlaars etc..)

Part I: The Surface Neumann G-Function

The surface Neumann G-function, G_s, is central to the analysis:

$$\triangle G_s = \frac{1}{|\Omega|}\,, \quad x \in \Omega\,; \qquad \partial_r G_s = \delta(\cos\theta - \cos\theta_j)\delta(\phi - \phi_j)\,, \quad x \in \partial\Omega\,,$$

Lemma: *Let* $\cos\gamma = x \cdot x_j$ *and* $\int_\Omega G_s\, dx = 0$. *Then* $G_s = G_s(x; x_j)$ *is*

$$G_s = \frac{1}{2\pi|x - x_j|} + \frac{1}{8\pi}(|x|^2 + 1) + \frac{1}{4\pi}\log\left[\frac{2}{1 - |x|\cos\gamma + |x - x_j|}\right] - \frac{7}{10\pi}\,.$$

Define the matrix $\mathcal{G}_s$ using $R = -\frac{9}{20\pi}$ and $G_{sij} \equiv G_s(x_i; x_j)$ as

$$\mathcal{G}_s \equiv \begin{pmatrix} R & G_{s12} & \cdots & G_{s1N} \\ G_{s21} & R & \cdots & G_{s2N} \\ \vdots & \vdots & \ddots & \vdots \\ G_{sN1} & \cdots & G_{sN,N-1} & R \end{pmatrix},$$

Remark: As $x \to x_j$, G_s has a subdominant logarithmic singularity:

$$G_s(x; x_j) \sim \frac{1}{2\pi|x - x_j|} - \frac{1}{4\pi}\log|x - x_j| + R + o(1)\,.$$

Part I: Main Result for $\bar{v}$

__Principal Result__: *For $\varepsilon \to 0$, and for N circular traps of radii εa_j centered at x_j, for $j = 1, \ldots, N$, the averaged MFPT $\bar{v}$ satisfies*

$$\bar{v} = \frac{|\Omega|}{2\pi\varepsilon D N\bar{c}} \left[1 + \varepsilon \log\left(\frac{2}{\varepsilon}\right) \frac{\sum_{j=1}^{N} c_j^2}{2N\bar{c}} + \frac{2\pi\varepsilon}{N\bar{c}} p_c(x_1, \ldots, x_N) \right.$$
$$\left. - \frac{\varepsilon}{N\bar{c}} \sum_{j=1}^{N} c_j \kappa_j + O(\varepsilon^2 \log \varepsilon) \right] .$$

Here $c_j = 2a_j/\pi$ is the capacitance of the j^{th} circular absorbing window of radius εa_j, $\bar{c} \equiv N^{-1}(c_1 + \ldots + c_N)$, $|\Omega| = 4\pi/3$, and κ_j and p_c are

$$\kappa_j = \frac{c_j}{2} \left[2\log 2 - \frac{3}{2} + \log a_j \right] ; \qquad p_c(x_1, \ldots, x_N) \equiv \mathcal{C}^t \mathcal{G}_s \mathcal{C} .$$

In the quadratic form for p_c, we label $\mathcal{C}^t = (c_1, \ldots, c_N)$.

Remarks: 1) A similar result holds for non-circular traps. 2) The logarithmic term in ε arises from the subdominant singularity in G_s.

Part I: Main Result for $\bar{v}$

Corollary: (CWS): For N circular traps of a common radius ε (for which $c_j = 2/\pi$ and $a_j = 1$), then a three-term expansion is

$$\bar{v} = \frac{|\Omega|}{4\varepsilon D N} \Big[1 + \frac{\varepsilon}{\pi} \log\left(\frac{2}{\varepsilon}\right) + \frac{\varepsilon}{\pi}\left(-\frac{9N}{5} + 2(N-2)\log 2 + \frac{3}{2} + \frac{4}{N}\mathcal{H}(x_1,\ldots,x_N) \right) + \mathcal{O}(\varepsilon^2 \log \varepsilon) \Big] ,$$

with discrete energy $\mathcal{H}(x_1,\ldots,x_N)$ given by

$$\mathcal{H}(x_1,\ldots,x_N) = \sum_{i=1}^{N}\sum_{k>i}^{N} \left(\frac{1}{|x_i - x_k|} - \frac{1}{2}\log|x_i - x_k| - \frac{1}{2}\log\left(2 + |x_i - x_k|\right) \right) .$$

- **Key point:** To minimize $\bar{v}$, we must minimize $\mathcal{H}$. This discrete energy generalizes the Coulombic or logarithmic energies of (classical) Fekete points. Extra term in $\mathcal{H}$ involves surface diffusion.
- **Ref: [CWS]:** *A. Chevaikov, M.J. Ward, R. Straube, An Asymptotic Analysis of the Mean First Passage Time for Narrow Escape Problems: SIAM J. Multiscale Modeling and Simulation: Part II The Sphere,* **8**, *(2010), pp. 836–870.*

Part I: Key Steps in Derivation

- Asymptotic expansion of global (outer) solution and local (inner solutions near each trap.
- Tangential-normal coordinate system used near each trap.
- The Neumann G-function has a subdominant logarithmic singularity on the boundary (related to surface diffusion). This fact requires adding “logarithmic switchback terms in ε” in the outer expansion (ubiquitous in Low Reynolds number flow problems)
- The leading-order local solution is the tangent plane approximation and yields electrified disk problem in a half-space, with capacitance c_j.
- **Key:** Need corrections to the tangent plane approximation in the inner region, i.e. near the trap. This higher order correction term in the inner expansion satisfies a Poission type problem. The far-field behavior of this inhomogeneous problem is a monopole term and determines κ_j.
- Asymptotic matching and solvability conditions (Divergence theorem) determine v and $\bar{v}$

Part I: Numerical Validation of $\bar{v}$

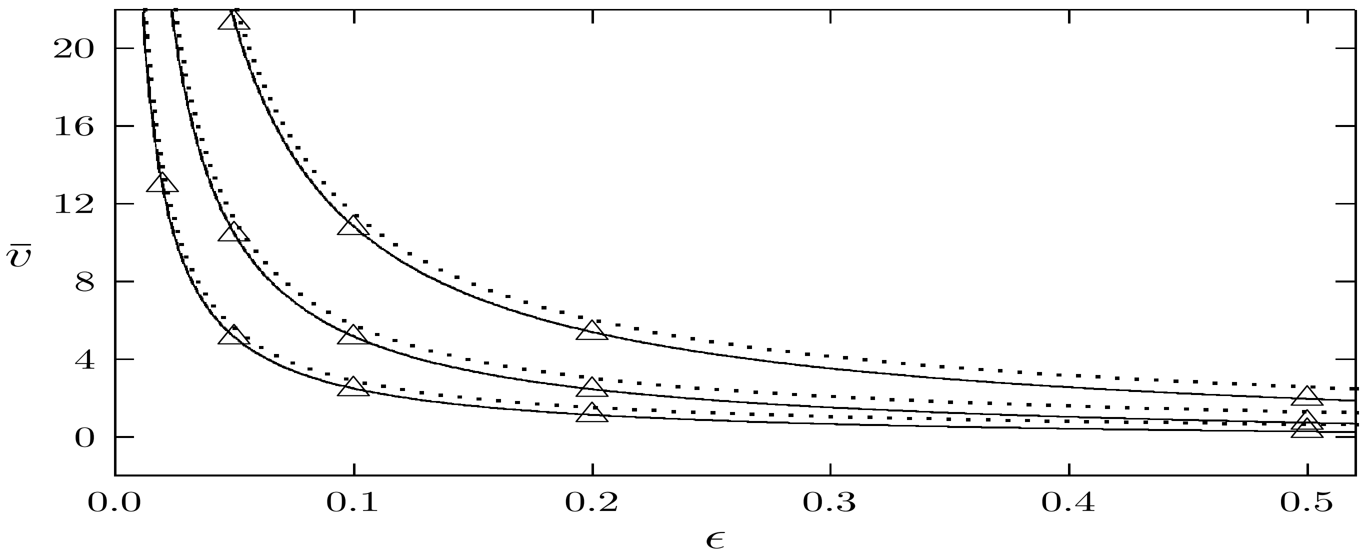

Plot: $\bar{v}$ vs. ε with $D = 1$ and either $N = 1, 2, 4$ equidistantly spaced circular windows of radius ε. **Solid:** 3-term expansion. **Dotted:** 2-term expansion. **Discrete:** COMSOL. **Top:** $N = 1$. **Middle:** $N = 2$. **Bottom:** $N = 4$.

	$N = 1$			$N = 2$			$N = 4$		
ε	$\bar{v}_2$	$\bar{v}_3$	$\bar{v}_n$	$\bar{v}_2$	$\bar{v}_3$	$\bar{v}_n$	$\bar{v}_2$	$\bar{v}_3$	$\bar{v}_n$
0.02	53.89	53.33	52.81	26.95	26.42	26.12	13.47	13.11	12.99
0.05	22.17	21.61	21.35	11.09	10.56	10.43	5.54	5.18	5.12
0.10	11.47	10.91	10.78	5.74	5.21	5.14	2.87	2.51	2.47
0.20	6.00	5.44	5.36	3.00	2.47	2.44	1.50	1.14	1.13
0.50	2.56	1.99	1.96	1.28	0.75	0.70	0.64	0.28	0.30

Part I: Numerical Validation of $\bar{v}$

Remark: For $\varepsilon = 0.5$ and $N = 4$, traps occupy $\approx 20\%$ of the surface. Yet, the 3-term asymptotics for $\bar{v}$ differs from COMSOL by only $\approx 7.5\%$.

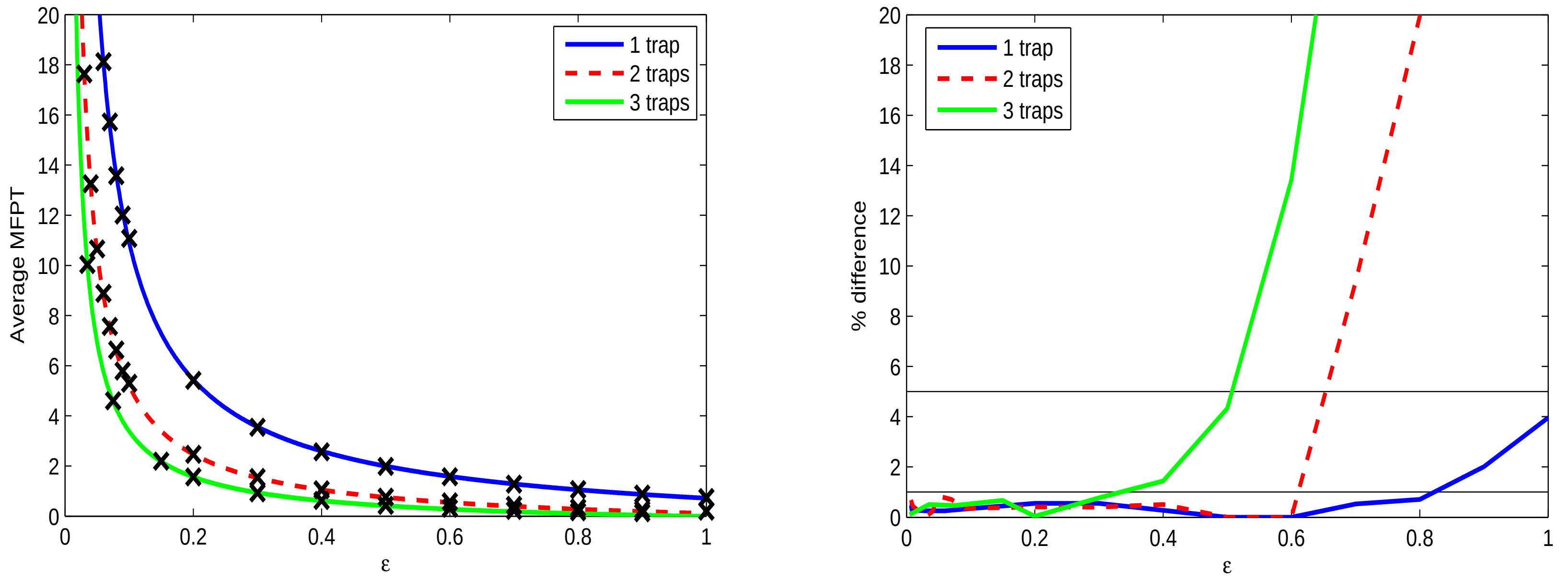

Fig: $\bar{v}$ vs. trap radius ε for $D = 1$ for one, two, and three traps equally spaced on the equator: curves (asymptotics), crosses (full numerics).

- For one trap, we get only 1% error for a trap of radius $\varepsilon \lesssim 0.8$, i.e. $\varepsilon^2/4 \times 100 = 16\%$ percent surface trap area fraction.
- For 3 traps, 1% error when $\varepsilon \lesssim 0.3$, which is 6.8% percent surface trap area fraction.

Part I: Fragmentation/Location of Traps

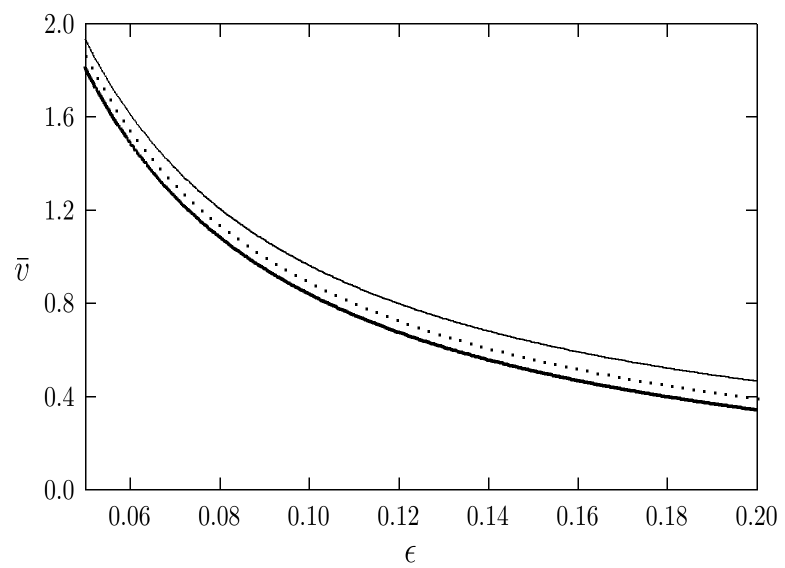

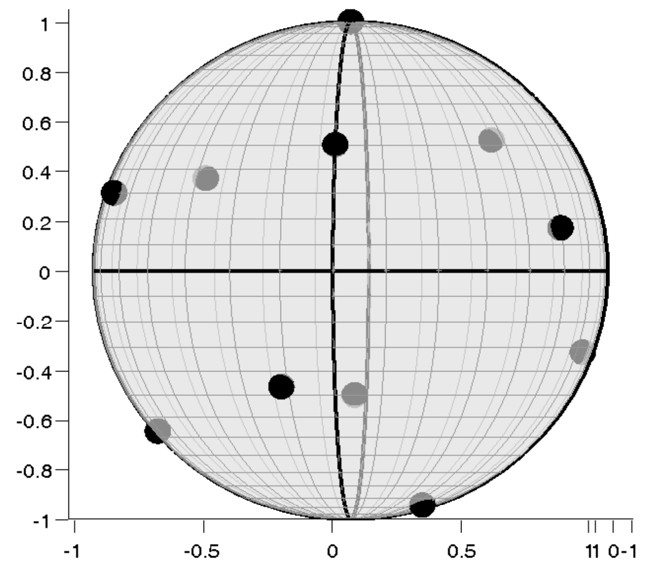

Plot: $\bar{v}(\varepsilon)$ for $D = 1$, $N = 11$, and three trap configurations. **Heavy:** global minimum of $\mathcal{H}$ (right figure). **Solid:** equidistant points on equator. **Dotted:** random.

- The effect of trap location is still rather significant.
- For $\varepsilon = 0.1907$, $N = 11$ traps occupy $\approx 10\%$ of surface area. The optimal arrangement gives $\bar{v} \approx 0.368$. For a single large trap with a 10% surface area, $\bar{v} \approx 1.48$; a result 3 times larger. Thus, trap fragmentation effects are important.

Part I: Discrete Optimization Problem I

Goal: Compare optimal energies and point arrangements of $\mathcal{H}$ with those of classic Coulomb or Logarithmic energies

$$\mathcal{H}_{\mathrm{C}} = \sum_{i=1}^{N} \sum_{j>i}^{N} \frac{1}{|x_i - x_j|}, \quad \mathcal{H}_{\mathrm{L}} = -\sum_{i=1}^{N} \sum_{j>i}^{N} \log|x_i - x_j|.$$

Numerics: Extended Cutting Angle Method: Implemented for $N \leq 65$ in open software library GANSO by A. Cheviakov, R. Spiteri, S. Richards.

N=5 **N=7** **N=12** **N=16**

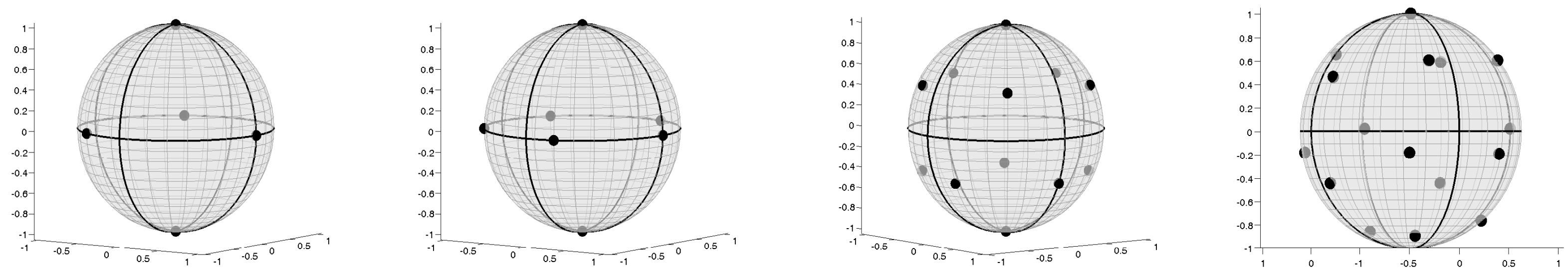

- Optimal $\mathcal{H}$ grows more slowly with N than for other discrete energies.
- For $N = 2, \ldots, 20$ optimal point arrangments coincide (proof?) Does agreement persist for large values of N?.

Part I: Discrete Optimization Problem II

OPTIMAL ENERGIES: (Computations by R. Spiteri and A. Cheviakov)

N	$\mathcal{H}$	$\mathcal{H}_{\mathrm{C}}$	$\mathcal{H}_{\mathrm{L}}$
3	-1.067345	1.732051	-1.647918
4	-1.667180	3.674234	-2.942488
5	-2.087988	6.474691	-4.420507
6	-2.581006	9.985281	-6.238324
7	-2.763658	14.452978	-8.182476
8	-2.949577	19.675288	-10.428018
9	-2.976434	25.759987	-12.887753
10	-2.835735	32.716950	-15.563123
11	-2.456734	40.596450	-18.420480
12	-2.161284	49.165253	-21.606145
16	1.678405	92.911655	-36.106152
20	8.481790	150.881571	-54.011130
25	21.724913	243.812760	-80.997510
30	40.354439	359.603946	-113.089255
35	64.736711	498.569272	-150.192059
40	94.817831	660.675278	-192.337690
45	130.905316	846.188401	-239.453698
50	173.078675	1055.182315	-291.528601
55	221.463814	1287.772721	-348.541796
60	275.909417	1543.830401	-410.533163
65	336.769710	1823.667960	-477.426426

Scaling Law for Optimum Point

For $N \gg 1$, the optimal $\mathcal{H}$ has the scaling law

$$\mathcal{H} \approx \mathcal{F}(N) \equiv \frac{N^2}{2} \log\left(\frac{e}{2}\right) + b_1 N^{3/2} + N\left(b_2 \log N + b_3\right) + b_4 N^{1/2} + b_5 \log N + b_6 \,,$$

where a least-squares fit to the optimal energy yields

$$b_1 \approx -0.5668\,, \quad b_2 \approx 0.0628\,, \quad b_3 \approx -0.8420\,,$$
$$b_4 \approx 3.8894\,, \quad b_5 \approx -1.3512\,, \quad b_6 \approx -2.4523\,.$$

Scaling Law For $\bar{v}$: For $1 \ll N \ll 1/\varepsilon$, the optimal average MFPT $\bar{v}$, in terms of the trap surface area fraction $f = N\varepsilon^2/4$, satisfies

$$\bar{v} \sim \frac{|\Omega|}{8D\sqrt{fN}} \left[1 - \frac{\sqrt{f/N}}{\pi} \log\left(\frac{4f}{N}\right) + \frac{2\sqrt{fN}}{\pi}\left(\frac{1}{5} + \frac{4b_1}{\sqrt{N}}\right)\right].$$

Part I: Fragmentation of the Trap Set

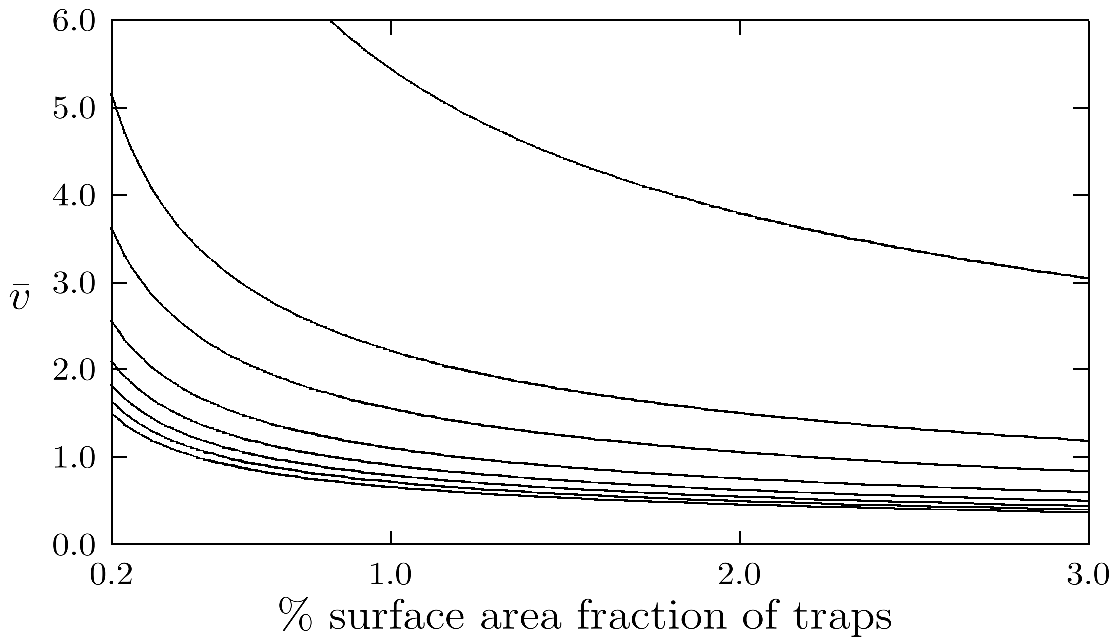

Plot: averaged MFPT $\bar{v}$ versus % trap area fraction for $N = 1, 5, 10, 20, 30, 40, 50, 60$ (top to bottom) at optimal trap locations.

- **Fragmentation** of traps on the sphere is a significant factor for small N.
- **Only a minimal benefit** by increasing N when N is already large.
- **Q1:** Derive a rigorous scaling law for optimal $\mathcal{H}$ when $N \gg 1$.
- **Q2:** Does the limiting result from $\mathcal{H}$ approach a homogenization theory result in the dilute trap area limit?

Part II: MFPT on the Sphere Surface

Consider Brownian motion on the surface of a sphere. The MFPT satisfies

$$\triangle_s v = -\frac{1}{D}\,, \qquad x \in \Omega_\varepsilon \equiv \Omega \backslash \cup_{j=1}^{N} \Omega_{\varepsilon_j}\,,$$

$$v = 0\,, \quad x \in \partial\Omega_{\varepsilon_j}\,; \qquad \bar{v} \sim \frac{1}{|\Omega_\varepsilon|}\int_{\Omega_\varepsilon} v\, ds\,.$$

Here Ω is the unit sphere, Ω_{ε_j} are localized non-overlapping circular traps of radius $O(\varepsilon)$ on Ω centered at x_j with $|x_j| = 1$ for $j = 1, \ldots, N$.

Eigenvalue Problem: The corresponding eigenvalue problem is

$$\triangle_s \psi + \lambda\psi = 0\,, \quad x \in \Omega_\varepsilon \equiv \Omega \backslash \cup_{j=1}^{N} \Omega_{\varepsilon_j}\,,$$

$$\psi = 0\,, \quad x \in \partial\Omega_{\varepsilon_j}\,; \quad \int_{\Omega_\varepsilon} \psi^2\, ds = 1\,.$$

- **Goal:** Calculate the principal eigenvalue λ_1 in the limit $\varepsilon \to 0$. Note that $\bar{v} \sim 1/(D\lambda_1)$ as $\varepsilon \to 0$. What is the effect of the trap locations?
- **Ref: [CSW]** D. Coombs, R. Straube, MJW, *"Diffusion on a Sphere with Traps..."*, SIAP **70**(1), (2009), pp. 302–332.

Part II: Elliptic Fekete Points

Elliptic Fekete Points are points that globally minimize the logarithmic energy $\mathcal{H}_L$ on the unit sphere

$$\mathcal{H}_L(x_1, \ldots, x_N) = -\sum_{j=1}^{N} \sum_{k>j}^{N} \log |x_j - x_k| \,, \quad |x_j| = 1 \,.$$

(References: Smale and Schub, Saff, Sloane, Kuijlaars, D. Boal, P. Palffy-Muhoray,...)

Key Question: Are elliptic Fekete points related to the configuration of traps that minimize the average MFPT $\bar{v}$ for diffusion on the sphere?

Part II: MFPT Two-Term Asymptotics

An asymptotic analysis yields (**Ref: [CSW]**):

<u>**Principal Result**</u>: *Consider N perfectly absorbing circular traps of a common radius $\varepsilon \ll 1$ centered at x_j, for $j = 1, \ldots, N$ on S. Then, the asymptotics for the MFPT v in the "outer" region $|x - x_j| \gg O(\varepsilon)$ for $j = 1, \ldots, N$ is*

$$v(x) = -2\pi \sum_{j=1}^{N} A_j G(x; x_j) + \bar{v} \,, \qquad \chi \equiv \frac{1}{4\pi} \int_S v \, ds \,,$$

where A_j for $j = 1, \ldots, N$, with $\mu \equiv -1/\log \varepsilon$ is

$$A_j = \frac{2}{ND} \left[1 + \mu \sum_{\substack{i=1 \\ i \neq j}}^{N} \log |x_i - x_j| - \frac{2\mu}{N} p(x_1, \ldots, x_N) + O(\mu^2) \right] \,.$$

The averaged MFPT $\bar{v}$ is given asymptotically by

$$\bar{v} = \frac{2}{ND\mu} + \frac{1}{D} \left[(2 \log 2 - 1) + \frac{4}{N^2} p(x_1, \ldots, x_N) \right] + O(\mu) \,.$$

Part II: MFPT Two-Term Asymptotics

Here the discrete energy $p(x_1, \ldots, x_N)$ *is the logarithmic energy*

$$p(x_1, \ldots, x_N) \equiv -\sum_{i=1}^{N} \sum_{j>i}^{N} \log |x_i - x_j| \, .$$

The Neumann Green function $G(x; x_0)$ that appears satisfies

$$\triangle_s G = \frac{1}{4\pi} - \delta(x - x_0) \, , \quad x \in S \, ; \quad \int_S G \, ds = 0$$

G is 2π periodic in ϕ and smooth at $\theta = 0, \pi$.

It is given analytically by

$$G(x; x_0) = -\frac{1}{2\pi} \log |x - x_0| + R \, , \qquad R \equiv \frac{1}{4\pi} \left[2 \log 2 - 1 \right] \, .$$

Remark: G appears in various studies of the motion of fluid vortices on the surface S of a sphere (P. Newton, S. Boatto, etc..).

Part I: MFPT Two-Term Asymptotics

Corollary: *For N identical perfectly absorbing traps of a common radius ε centered at x_j, for $j = 1, \ldots, N$, on S, the principal eigenvalue has asymptotics, with* $\mu \equiv -1/\log \varepsilon$

$$\lambda(\varepsilon) \sim \frac{\mu N}{2} + \mu^2 \left[-\frac{N^2}{4} (2\log 2 - 1) - p(x_1, \ldots, x_N) \right] + O(\mu^3)\,.$$

- **Key Point:** $\lambda(\varepsilon)$ is maximized and $\bar{v}$ minimized at the minumum point of p, i.e. at the elliptic Fekete points for the sphere.
- Can readily adapt the analysis to treat the case of N partially absorbing traps of different radii (see **[CSW,2009]**).
- For $N = 1$, v and λ_1 can be found from ODE problems, and we reproduce old results of Weaver (1983), Chao et. al. (1981), Biophys. J., and Lindeman and Laufenburger, Biophys, J. (1986)). In particular,

$$\lambda(\varepsilon) \sim \frac{\mu}{2} + \frac{\mu^2}{4} (1 - 2\log 2)\ .$$

Part II: Summing the Logs

Can formulate a problem involving the Helmholtz Green function on the sphere that sums the infinite logarithmic expansion for $\lambda(\varepsilon)$. It reads as:

Principal Result: *Consider N perfectly absorbing traps of a common radius ε for $j = 1, \ldots, N$. Let $\nu(\varepsilon)$ be the smallest root of the transcendental equation*

$$\mathrm{Det}\,(I + 2\pi\mu\mathcal{G}_h) = 0\,, \qquad \mu = -\frac{1}{\log \varepsilon}\,.$$

Here $\mathcal{G}_h$ is the Helmholtz Green function matrix with matrix entries

$$\mathcal{G}_{hjj} = R_h(\nu)\,; \qquad \mathcal{G}_{hij} = -\frac{1}{4\sin(\pi\nu)} P_\nu\left(\frac{|x_j - x_i|^2}{2} - 1\right)\,, \quad i \neq j\,.$$

Then, with an error of order $O(\varepsilon)$, we have $\lambda(\varepsilon) \sim \nu(\nu+1)$.

- $P_\nu(z)$ is the Legendre function of the first kind, with regular part

$$R_h(\nu) \equiv -\frac{1}{4\pi}\left[-2\log 2 + 2\gamma + 2\psi(\nu+1) + \pi\cot(\pi\nu)\right]\,,$$

where γ is Euler's constant and ψ is the Di-Gamma function.

Part I: Validation of Asymptotics

We validate our two-term and summing logs asymptotic theory by comparing with full numerical results

	5 random traps			2 antipodal traps		
ε	λ	λ^*	λ_2	λ	λ^*	λ_2
0.02	0.7918	0.7894	0.7701	0.2458	0.2451	0.2530
0.05	1.1003	1.0991	1.0581	0.3124	0.3121	0.3294
0.1	1.5501	1.5452	1.4641	0.3913	0.3903	0.4268
0.2	2.5380	2.4779	2.3278	0.5177	0.5110	0.6060

Legend: λ (COMSOL); $\lambda^\star$ (Summing Logs); λ_2 (2-term).

Note: For $\varepsilon = 0.2$ and $N = 5$, we get 5% trap area fraction. The agreement is still very good: 2.4% error (summing logs) and 8.3% error (2-term).

Part II: Effect of Trap Locations

EFFECT OF SPATIAL ARRANGEMENT OF $N = 4$ IDENTICAL TRAPS:

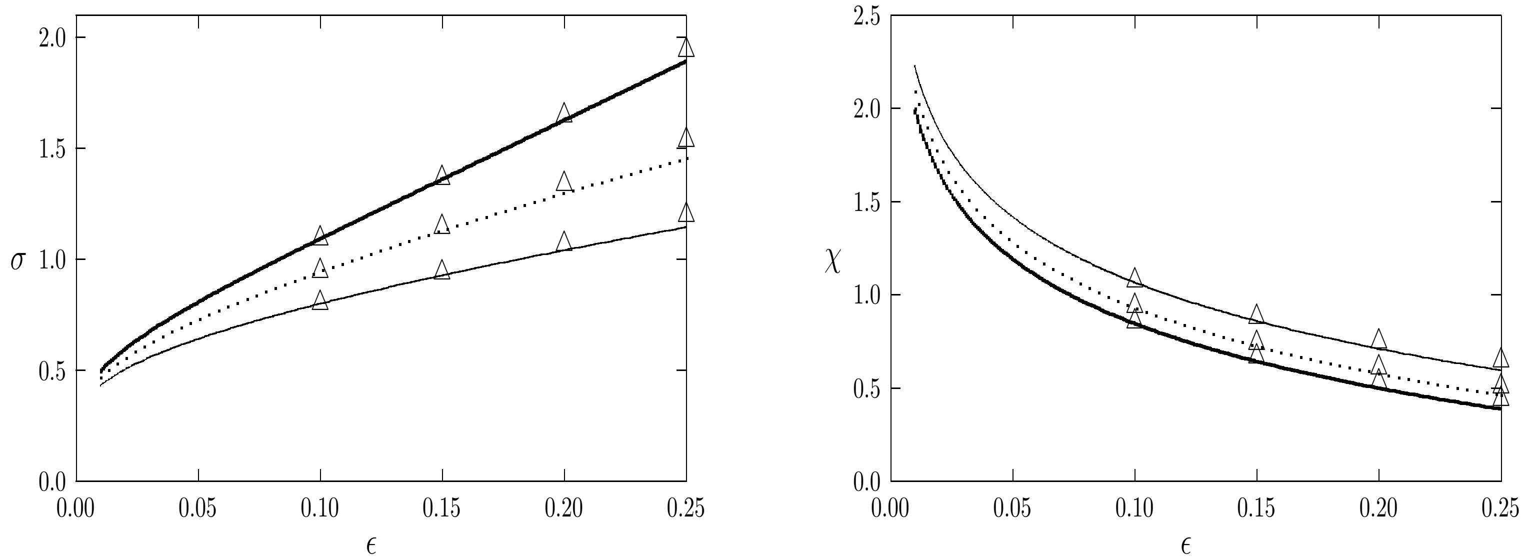

Note: $\varepsilon = 0.1$ corresponds to 1% trap surface area fraction.

Fig: Results for $\lambda(\varepsilon)$ (left) and $\bar{v}(\varepsilon)$ (right) for three different 4-trap patterns with perfectly absorbing traps and a common radius ε. **Heavy solid:** $(\theta_1, \phi_1) = (0, 0)$, $(\theta_2, \phi_2) = (\pi, 0)$, $(\theta_3, \phi_3) = (\pi/2, 0)$, $(\theta_4, \phi_4) = (\pi/2, \pi)$; **Solid:** $(\theta_1, \phi_1) = (0, 0)$, $(\theta_2, \phi_2) = (\pi/3, 0)$, $(\theta_3, \phi_3) = (2\pi/3, 0)$, $(\theta_4, \phi_4) = (\pi, 0)$; **Dotted:** $(\theta_1, \phi_1) = (0, 0)$, $(\theta_2, \phi_2) = (2\pi/3, 0)$, $(\theta_3, \phi_3) = (\pi/2, \pi)$, $(\theta_4, \phi_4) = (\pi/3, \pi/2)$. The marked points are computed from finite element package COMSOL.

Part II: A Scaling Law

For $N \to \infty$, the optimal energy for the discrete variational problem associated with elliptic Fekete points gives

$$\max\left[-p(x_1,\ldots,x_N)\right] \sim \frac{1}{4}\log\left(\frac{4}{e}\right)N^2 + \frac{1}{4}N\log N + l_1 N + l_2\,, \quad N \to \infty\,,$$

with $l_1 = 0.02642$ and $l_2 = 0.1382$.

Ref: E. A. Rakhmanov, E. B. Saff, Y. M. Zhou, (1994); B. Bergersen, D. Boal, P. Palffy-Muhoray, J. Phys. A: Math Gen., **27**, No. 7, (1994).

This yields a key scaling law for the minimum of the averaged MFPT:

Principal Result: *For $N \gg 1$, and N circular disks of common radius ε, and with small trap area fraction $N(\pi\varepsilon^2) \ll 1$ with $|S| = 4\pi$, then*

$$\min \bar{v} \sim \frac{1}{ND}\left[-\log\left(\frac{\sum_{j=1}^{N}|\Omega_{\varepsilon_j}|}{|S|}\right) - 4l_1 - \log 4 + O(N^{-1})\right].$$

Part II: Biophysical Application

Application: Estimate the averaged MFPT T for a surface-bound molecule to reach a molecular cluster on a spherical cell.

Physical Parameters: The diffusion coefficient of a typical surface molecule (e.g. LAT) is $D \approx 0.25\mu$m^2/s. Take $N = 100$ (traps) of common radius 10nm on a cell of radius 5μm. This gives a 1% trap area fraction:

$$\varepsilon = 0.002\,, \qquad N\pi\varepsilon^2/(4\pi) = 0.01\,.$$

Scaling Law: The scaling law gives an asymptotic lower bound on the averaged MFPT. For $N = 100$ traps, the bound is 7.7s, achieved at the elliptic Fekete points.

One Big Trap: As a comparison, for one big trap of the same area the averaged MFPT is 360s, which is very different.

Bounds: Therefore, for any other arrangement, 7.7s $< T < 360$s.

Conclusion: Both the Spatial Distribution and Fragmentation Effect of Localized Traps are Rather Significant even at Small Trap Area Fraction

Part III: Spot Patterns in RD Systems

Spatially localized solutions can occur for singularly perturbed RD models

$$u_t = \varepsilon^2 \triangle u + f(u,v)\,; \qquad \tau v_t = D \triangle v + g(u,v)\,, \qquad x \in \Omega \in \mathbb{R}^2\,.$$

Assume semi-strong interactions for which $\varepsilon \ll 1$ and $D = \mathcal{O}(1)$.

Key: Since $\varepsilon \ll 1$, v can be localized in space as a spot pattern, i.e. concentration at a discrete set of points.

Some Well-Known RD systems:

- **Gray-Scott Model:** (Pearson, Science 1993, Muratov scaling (1996))

$$f(u,v) = -u + Avu^2\,, \qquad f(u,v) = (1-v) - vu^2\,.$$

- **Schnakenburg Model:** $f(u,v) = -u + vu^2$ and $g(u,v) = a - vu^2$.
- **GM Model:** $f(u,v) = -u + u^2/u$ and $g(u,v) = -v + u^2$.
- **Brusselator Model:** $f(u,v) = E - (B+1)u + u^2 v$, $g(u,v) = Bu - u^2 v$.

Difficulties: No variational structure; Patterns are “far-from- equilibrium”. Turing and weakly nonlinear theories are not applicable.

Part III: Brusselator on the Unit Sphere

$$\partial_T U = \varepsilon_0^2 \, \Delta_S \, U + \hat{E} - (B+1)U + U^2 V \,, \quad \partial_T V = D \, \Delta_S \, V + BU - U^2 V \,.$$

where $\varepsilon_0^2 \equiv D_U / L^2$, $D \equiv D_V / L^2$, and L is the radius of the sphere. Here Δ_S is the surface Laplacian for the unit sphere.

Asymptotic Limit: where $\varepsilon_0 \ll 1$ and $\hat{E} = \mathcal{O}(\varepsilon_0)$.

Introduce new variables:

$$T = \frac{t}{B+1} \,, \qquad U = \frac{\sqrt{(B+1)D}}{\varepsilon_0} u \,, \qquad V = \frac{B}{\sqrt{(B+1)D}} \varepsilon_0 v \,.$$

This yields non-dimensional Brusselator Model:

$$u_t = \varepsilon^2 \, \Delta_S \, u + \varepsilon^2 \mathrm{E} - u + f u^2 v \,, \qquad \tau v_t = \Delta_S \, v + \varepsilon^{-2} \left(u - u^2 v \right) \,.$$

with

$$\varepsilon \equiv \frac{\varepsilon_0}{\sqrt{B+1}} \,, \quad \tau \equiv \frac{(B+1)}{D} \,, \quad f \equiv \frac{B}{B+1} \,, \quad E \equiv \frac{\hat{E}}{\sqrt{(B+1)D}\varepsilon_0} \,.$$

Part III: Turing Stability Analysis

The spatially uniform state is $u_e = \varepsilon^2 \mathrm{E}/(1-f)$ and $v_e = (1-f)/(\varepsilon^2 \mathrm{E})$.

Turing-Type stability analysis: Introduce perturbation of the uniform state:

$$(u, v) = (u_e, v_e) + e^{\lambda t} Y_l^m(\theta, \phi)(\hat{u}, \hat{v}), \qquad k^2 \equiv l(l+1), \quad |m| \leq l.$$

For $\varepsilon \to 0$ and $f > 1/2$, the (wide) instability band where Re$(\lambda) > 0$ is $0 < k_{\text{low}} < k < k_{\text{up}} \sim \sqrt{2f-1}/\varepsilon$.

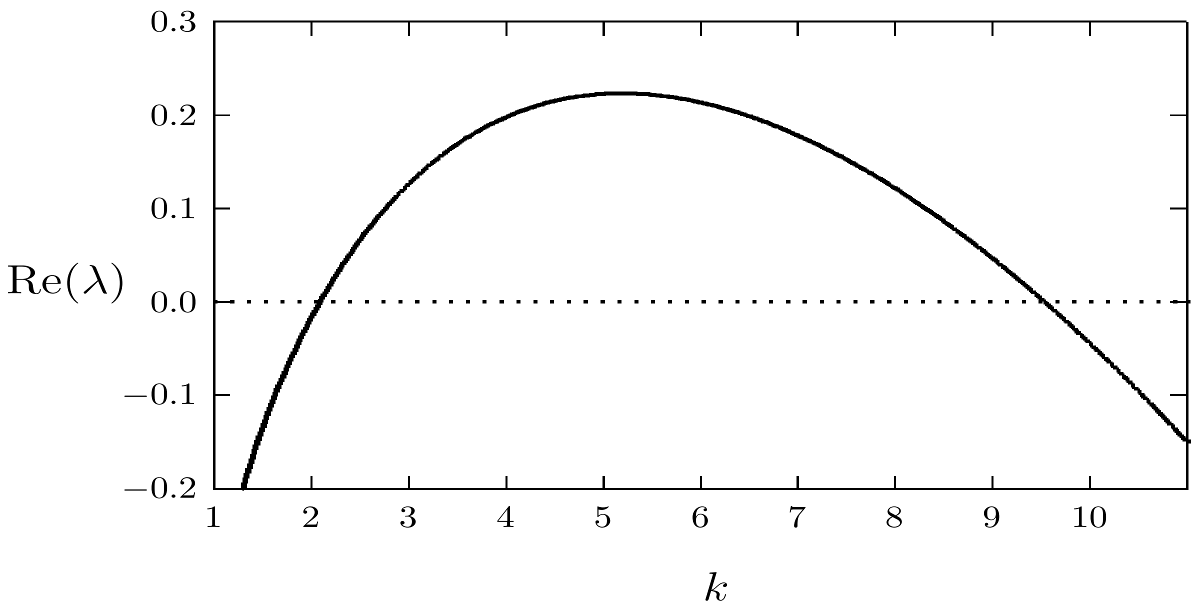

Plot: Re(λ) versus k for $f = 0.8$, $\varepsilon = 0.075$, and $\mathrm{E} = 2.5$.

Part III: Turing/Weakly Nonlinear Theory

Key: For $\varepsilon \ll 1$, any spherical harmonic $Y_l^m(\theta, \phi)$ with integers l and m satisfying $4.45 \leq l(l+1) \leq 91.6$ and $|m| \leq l$ is unstable. This gives $l = 2, \ldots, 9$.

Fundamental Difficulty: The linear stability problem with $f > 1/2$ and $\varepsilon \ll 1$ is **highly degenerate** with many unstable modes of comparable growth rate.

Weakly Nonlinear Analysis: For $\varepsilon = \mathcal{O}(1)$ tune parameters to onset of instability. However, due to degeneracy of spherical harmonics, eigenspace of zero-eigenvalue crossing is large. This leads to large set of coupled nonlinear normal form ODE amplitude equations via equivariant bifurcation theory. Weakly nonlinear patterns are unstable (subcritical), but re-stabilize at a saddle node point after including cubic terms. (Chossat, Melbourne, Archive Rat. Mech. Anal. 1990; Callahan, Physica D, 2004; P. Matthews, Nonlinearity 2003, Phys. Rev. E. 2003).

Key Difficulty:

- Due to mode degeneracy, linear and weakly nonlinear analysis is of only limited use in predicting pattern development.

Part III: Brusselator Patterns (Numerics)

Set: $f = 0.8$, $\varepsilon = 0.075$, $\mathrm{E} = 6$. **Initial data is uniform state with 2% random pert.**

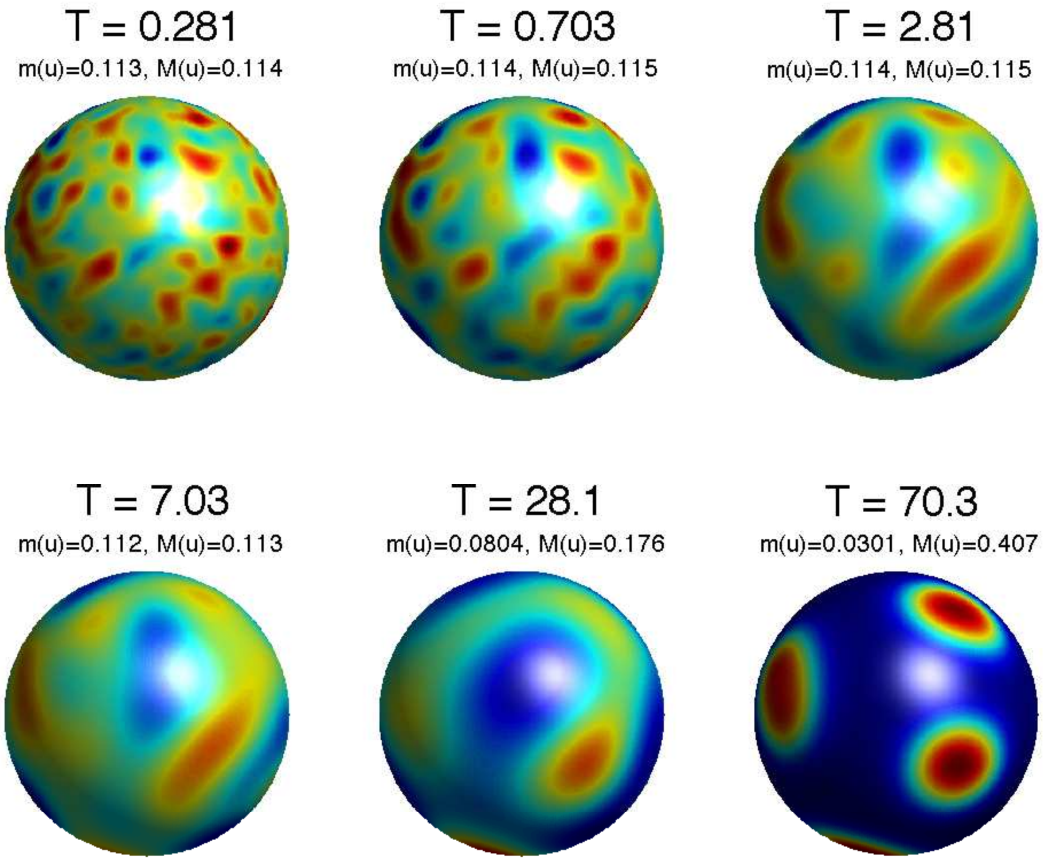

Numerics: "Closest Point Algorithms to Compute PDE's on Surfaces", by S. Ruuth (SFU) , C. McDonald (Oxford).

Initial Transient: very complicated due to interaction of many unstable modes, but leads to 8 localized spots.

Part III: Challenges and Questions

- **Challenge:** Develop a mathematical theory to analyze the existence, stability, and dynamics, of localized “far-from equilibrium” spot patterns.
- **Question 1:** Do such localized patterns undergo secondary instabilities on longer time-scales? (competition, self-replication, etc.)
- **Question 2:** Can one derive a reduced dynamical system for the locations of the spots? Any similarities to Eulerian point vortices?
- **Question 3:** Are steady-state spot patterns related to elliptic Fekete points?

Ref 1 (Quasi-Equilibria and Stability): I. Rozada, S. Ruuth, M.J. Ward, *The Stability of Localized Spot Patterns for the Brusselator on the Sphere*, SIADS, **13**(1), (2014), pp. 564–627.

Ref 2 (Slow Dynamics): P. Trinh, M.J. Ward, *Slow Spot Dynamics for Reaction-Diffusion Systems on the Sphere*, submitted Nov. 2014, Nonlinearity, (39 pages).

Part II: Self-Replication Instability

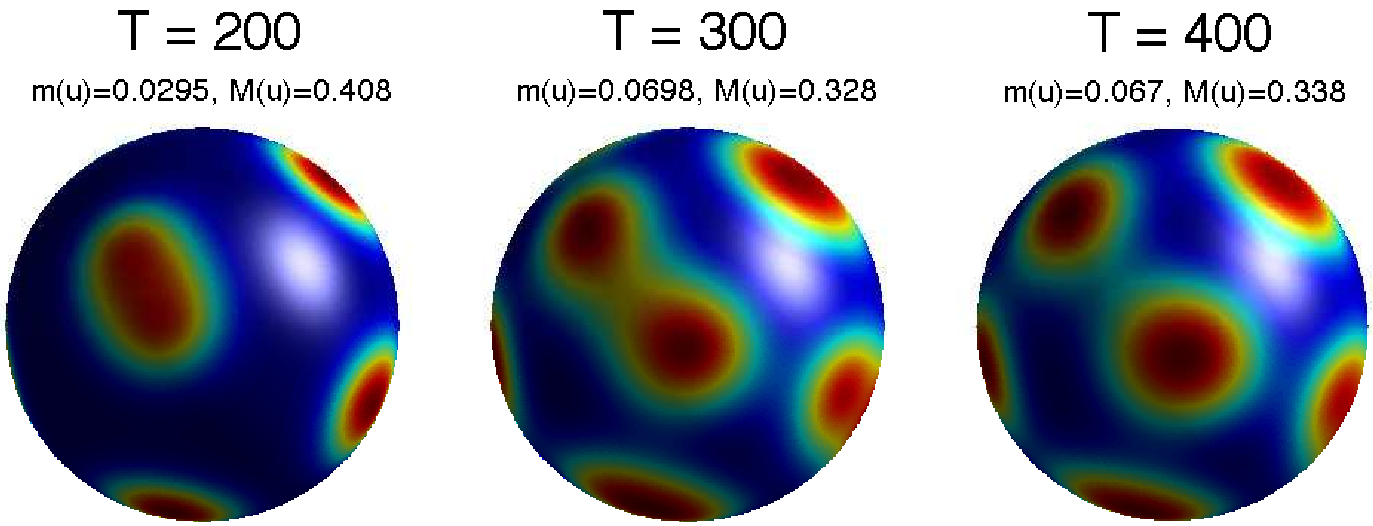

Plot: Solution at later times for $f = 0.8$, $\varepsilon = 0.075$. For $t \leq 70$ we take $\mathrm{E} = 6$. and then slowly increase E as $\mathrm{E} = \min(6 + 0.05(t - 70), 9)$. Spot self-replication occurs over a rather long time-scale due to dynamically-triggered bifurcation.

Spot self-replication (Another Example): Take $f = 0.7$, $\varepsilon = 0.06$, and $\mathrm{E} = 5.0$ for $0 < t < 50$. Increase the fuel E as $\mathrm{E} = 5.0 + \sigma(t - 50)$ with $\sigma = 0.05$ for $t \geq 50$. Roughly simultaneous spot splitting occurs. (Movie)

Part II: Quasi-Equilibria

Principal Result: *For $\varepsilon \to 0$, the quasi-equilibrium solution is given by an outer solution, valid away from the spots, and inner core solutions near each of of the spots centered at $\mathbf{x} = \mathbf{x}_j$ for $j = 1, \ldots, N$:*

$$u_{\text{qe}} \sim \varepsilon^2 \mathrm{E} + \sum_{i=1}^{N} U_{i,0}\left(\frac{|\mathbf{x} - \mathbf{x}_i|}{\varepsilon}\right), \qquad v_{\text{qe}} \sim \sum_{i=1}^{N} S_i L_i(\mathbf{x}) + \overline{v},$$

where $L_i(\mathbf{x}) \equiv \log|\mathbf{x} - \mathbf{x}_i|$, and $\overline{v}$ is a constant. The leading-order radially symmetric inner core solution, $U_{i,0}$, is defined on the tangent plane to the sphere near the spot at $\mathbf{x} = \mathbf{x}_i$. The spot strengths, S_i for $i = 1, \ldots, N$, satisfy the nonlinear algebraic system

$$\mathcal{N}(\mathbf{S}) \equiv \Big[\mathrm{I} - \nu(\mathrm{I} - \mathcal{E}_0)\mathcal{G}\Big]\mathbf{S} + \nu(\mathrm{I} - \mathcal{E}_0)\chi(\mathbf{S}) - \frac{2\mathrm{E}}{N}\mathbf{e} = \mathbf{0}.$$

Here I is the identity, $(\mathcal{E}_0)_{ij} = \frac{1}{N}$, $(\mathbf{S})_i = S_i$, $(\chi(\mathbf{S}))_i = \chi(S_i)$, $(\mathbf{e})_i = 1$, and $\nu = -1/\log\varepsilon$. The values of $\chi(S_i)$ are found by numerically solving a core problem. The Green's matrix $\mathcal{G}$ is a key quantity:

$$(\mathcal{G})_{ij} = \log|\mathbf{x}_i - \mathbf{x}_j| \equiv L_i(\mathbf{x}_j), \quad i \neq j; \qquad (\mathcal{G})_{ii} = 0.$$

Part III: Slow Spot Dynamics

Principal Result:*Let* $\varepsilon \to 0$. *Provided that there are no* $\mathcal{O}(1)$ *time-scale instabilities of the quasi-equilibrium spot pattern, the spot locations,* $\mathbf{x}_j(\sigma)$ *for* $j = 1, \ldots, N$*, with* $\sigma = \varepsilon^2 t$*, satisfy the ODE-DAE system*

$$\frac{d\mathbf{x_j}}{d\sigma} = \frac{2}{\mathcal{A}_j}\left(\mathrm{I} - \mathcal{Q}_j\right) \sum_{\substack{i=1 \\ i\neq j}}^{N} \frac{S_i \mathbf{x}_i}{|\mathbf{x}_i - \mathbf{x}_j|^2}\,, \qquad \mathcal{Q}_j \equiv \mathbf{x}_j \mathbf{x}_j^T\,, \qquad j = 1, \ldots, N\,.$$

coupled to the nonlinear algebraic constraint (NAS)

$$\mathcal{N}(\mathbf{S}) \equiv \Big[\mathrm{I} - \nu(\mathrm{I} - \mathcal{E}_0)\mathcal{G}\Big]\mathbf{S} + \nu(\mathrm{I} - \mathcal{E}_0)\chi(\mathbf{S}) - \frac{2\mathrm{E}}{N}\mathbf{e} = \mathbf{0}\,.$$

Here $\mathcal{A}_j = \mathcal{A}(S_j; f) < 0$ *is defined via an integral.*

Remarks:

- The matrix $I - \mathcal{Q}_j$ projects onto the unit sphere.
- If $\mathbf{x}_j$ is a solution then so is $\mathcal{R}\mathbf{x}_j$ where $\mathcal{R}$ is an orthogonal matrix.

Part III: The Core Problem

On the tangent plane near the j-th spot, we look for a locally radially symmetric core solution satisfying

$$\Delta_\rho U_{j0} - U_{j0} + f U_{j0}^2 V_{j0} = 0\,, \qquad \Delta_\rho V_{j0} + U_{j0} - U_{j0}^2 V_{j0} = 0\,,$$

$$U_{j0}'(0) = V_{j0}'(0) = 0\,; \quad U_{j0} \to 0\,, \quad V_{j0} \sim S_j \log \rho + \chi(S_j) + o(1) \text{ as } \rho \to \infty.$$

This problem determines $\chi(S_j)$.

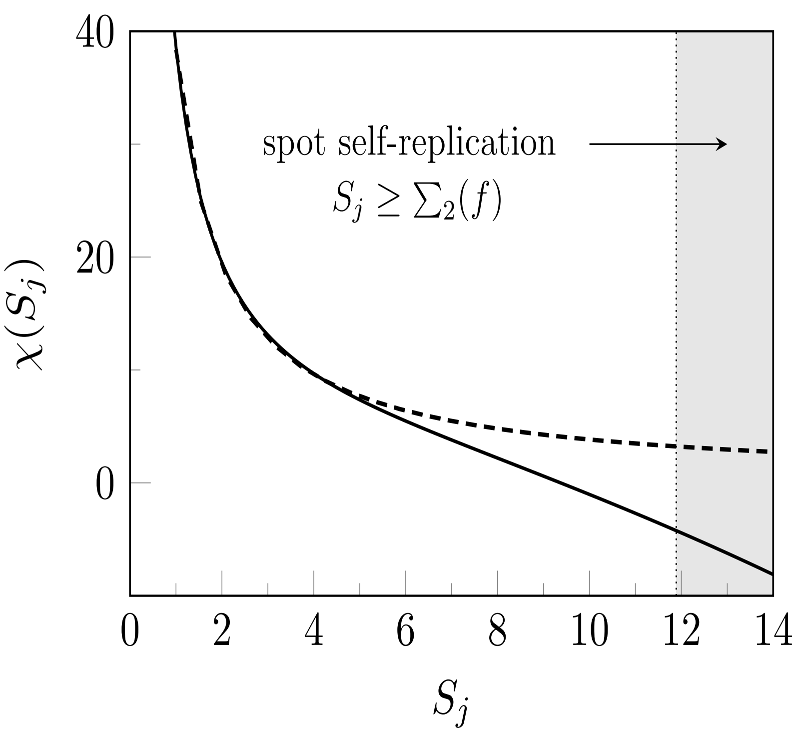

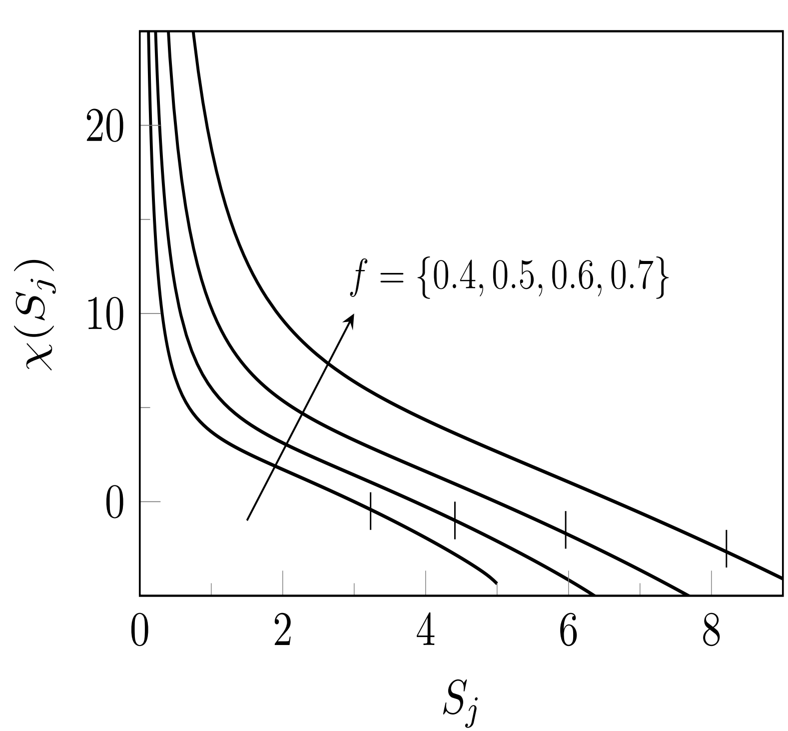

Part III: The Spot Strengths I

Common Source Strength Patterns: If the pattern $\{\mathbf{x}_1, \ldots, \mathbf{x}_N\}$ of spots are such that $\mathcal{G}\mathbf{e} = \kappa_1 \mathbf{e}$ then,

$$S_1 = S_2 =, \ldots, S_N = S_c \equiv \frac{2\mathrm{E}}{N}\,.$$

This property holds for spots equi-distantly placed on a ring, for all platonic solids, any two-spot pattern, and for twisted cuboids.

Q1: Determine all spatial configurations of spots for which this holds. Any relation to Elliptic Fekete Points?

A Key Link: If we set $S_j = S_c$ for all j in the dynamics, then stable equilibria of the dynamics are local minima of the discrete logarithmic energy

$$\mathcal{H}_L(x_1, \ldots, x_N) \equiv -\sum_{i=1}^{N}\sum_{j>i}^{N} \log|\mathbf{x}_i - \mathbf{x}_j|\,, \qquad |x_j| = 1\,, \quad j = 1, \ldots, N\,.$$

Proof: Use Lagrange multipliers and project to the sphere.

Part III: The Spot Strengths II

Elliptic Fekete points lead to a $\mathcal{G}$ matrix for which $\mathbf{e}$ is nearly an eigenvector. Q: Is there an asymptotic equipartition of the discrete logarithmic energy for large N?

Number of points N	$\|\|\xi - \mathbf{e}\|\|_2$
8	$6.0301e-16$
10	0.0216
20	0.0050
100	0.0029
120	0.0015

Table: Distance $\|\|\ldots\|\|_2$ between an eigenvector ξ of $\mathcal{G}$ and $\mathbf{e}$, both normalized, for different elliptic Fekete point configurations. A random distribution of 100 points on the sphere has a norm difference of 0.2512.

Part III: Steady-State Spot Patterns

For $N = 2, \ldots, 8$, for 50 randomly generated initial spot configurations we solved the ODE-DAE system to detect stable steady-states with large basins of attraction:

Results:

- **N=2:** two antipodal spots ($S_1 = S_2$)
- **N=3:** Three equally-spaced spots on a equator ($S_1 = S_2 = S_3$).
- **N=4:** Spots at vertices of a tetrahedron ($S_j = S_c$ for $j = 1, \ldots, 4$).
- **N=5,6,7:** Two antipodal spots, with $N - 2$ spots equally-spaced on the mid-plane. Two source strengths S_p and S_c.
- **N=8** Pattern is a 45° twisted cuboid consisting of two parallel planes, each containing four equally-spaced spots. The spots on the two planes are 45° phase-shifted. The ratio of the distance between neighboring spots on a ring to the perpendicular distance between the planes is approximately 0.967. This yields that the planes are at latitudes $\theta \approx 55.6^\circ$ and $\theta \approx 124.4^\circ$. ($S_j = S_c$ for $j = 1, \ldots, 8$). This is the elliptic Fekete point pattern for 8 particles.

Eight-Spot Pattern

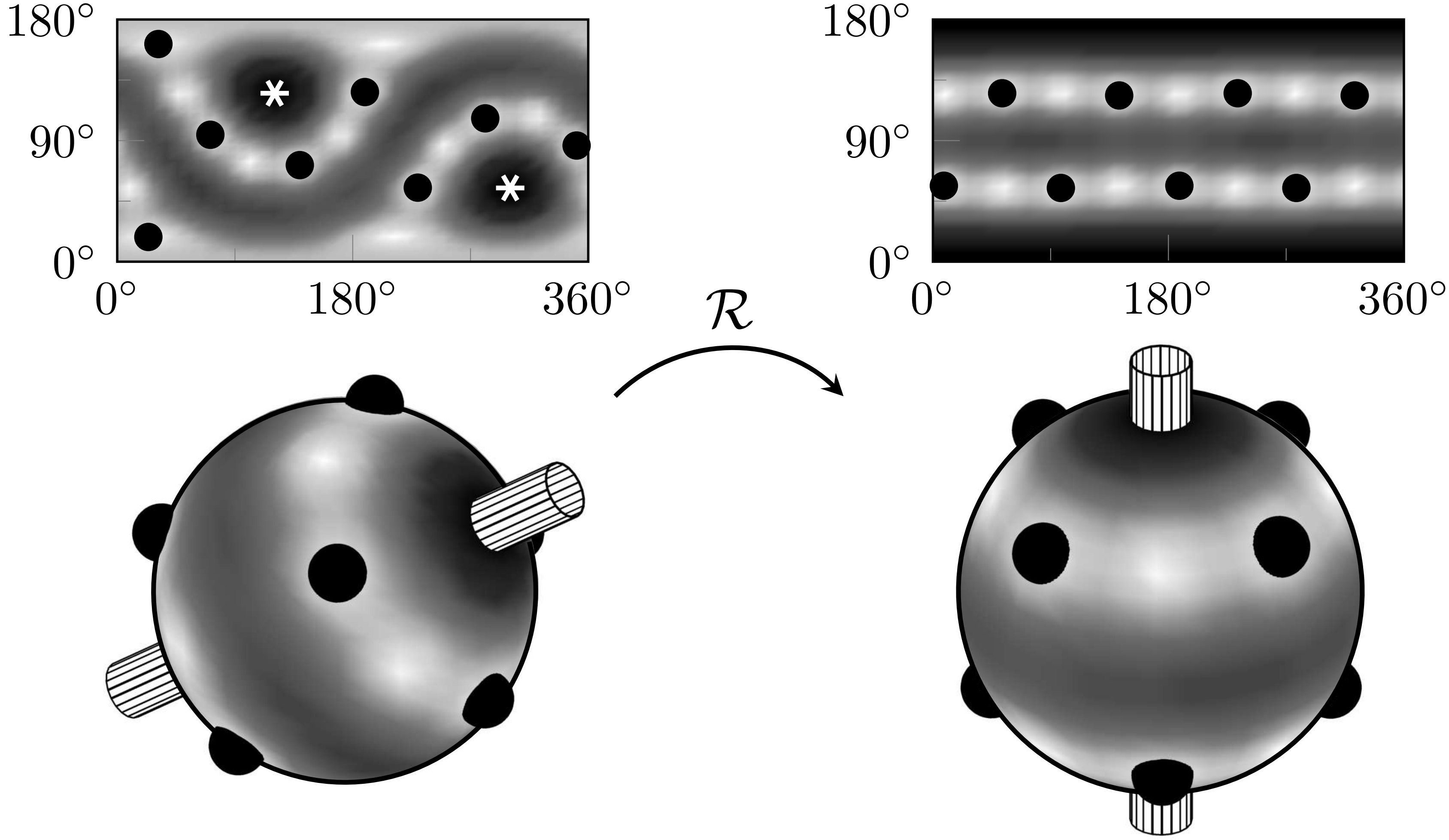

Left: The shading on the sphere and top (ϕ, θ) plane indicate with two asterisks a better location to place the polar axis of the sphere (marked by a cylinder). (Right) After an orthogonal transformation, $\mathcal{R}$, the rotated sphere in the (new) $(\bar{\phi}, \bar{\theta})$-plane shows two rings of four spots.

Final Remarks

- After an asymptotic reduction, all three problems lead to reduced problems involving discrete interacting particles.
- For the 3-D narrow escape problem, we have derived a new discrete energy. Study rigorously the asymptotics for large N for globally minimum energy states.
- For spot dynamics, use symmetry group analysis combined with ODE dynamics to classify the steady-state patterns for $N > 8$. In contrast to weakly nonlinear theory, this ODE-DAE dynamics gives a new approach for analyzing RD patterns on the sphere.
- Set $S_j = S_c$ for $j = 1, \ldots, N$. Does the ODE system provide a more tractable way to compute elliptic Fekete points?